Iraqi Journal of Physics, 2025 *Vol. 23, No.2, PP. 21-34*
https://doi.org/10.30723/ijp.v23i2.1310 *P-ISSN: 2070-4003*
E-ISSN: 2664-5548

Assessment of Climate Suitability with Land Cover Distribution for Amara City Using Remote Sensing Techniques

Hawazen Hassan Muslim[1*], Bassim M. Hashim[2] and Sundus A. Abdullah[1]
[1]*Department of Remote Sensing and GIS, College of Science, University of Baghdad, Baghdad, Iraq*
[2]*Research and Technology Center of Environment, Water and Renewable Energy, Scientific Research Commission, Ministry of Higher Education and Scientific Research, Baghdad, Iraq*
[*]Corresponding author: hawazenhassan892@gmail.com

Abstract
The current study used satellite data and geographic information systems to detect changes in land use and land cover and also studied climate factors, temperature, and humidity in Amara, located in the southeast of Iraq, from 1990 to 2022. The study aimed to calculate the land use land cover (LULC) using satellite images from Landsat 5 TM, Landsat 8 OLI, and Landsat 9 OLI2, also from the Meteorological Service; temperature and humidity data were used to calculate the Temperature-Humidity Index (THI). Iraq was one of the nations most exposed to the altering climate due to global warming and its effects. There was an urgent need to research climate change and land use in Amara City as temperatures rose and the city experienced drought and a shortage of rainfall. The findings showed that the percentage of urban areas increased noticeably from 38.2 to 69.8 km^2, the amount of vegetation increased slightly, and the barren areas were the highest. Low rainfall in the study area and high temperatures caused by global warming are two major variables affecting public safety. The main factors that affect the comfort of residents are temperature and humidity. The results of the climate suitability study also indicated that November and December are considered the most suitable months for the population, while the hottest and most unpleasant months were from the end of May to the beginning of September.

Article Info.

Keywords:
Land Use, Land Cover, Landsat, THI, Climatic Suitability.

Article history:
Received: May 31, 2024
Revised: Oct. 23, 2024
Accepted:Oct. 27, 2024
Published: Jun.01,2025

1. Introduction
One of the most main uses of remote sensing and Geographic Information System (GIS) techniques is the production of Land Use Land Cover (LULC) maps. The term "land use" refers to the goals of a land survey, which include urban development, agriculture, tourism, wildlife habitat preservation, and most domains in which humans are involved. The term "land cover" refers to the surface cover, including everything from flora, water, bare soil, and urban development [1, 2]. The land cover originally referred to the physical characteristics of the Earth's surface, including its types, surface and ground waters, and soil composition. Conversely, land use refers to how humans use of the land and its resources, including mining, logging, pastoralism, agriculture, and urbanization [3]. Leading environmental scales, change detection, global, regional, and local mapping are all made possible by the results of LULC mapping. One way to visualize the classification of remote sensing images is to use an unsupervised classification technique. It creates clusters based on the image's intrinsic spectral features that are similar. Next, it categorizes every cluster without offering any training examples [4]. Climate change is one of the worldwide challenges that is receiving a lot of attention due to its apparent impact on all living things; this is especially true now that Iraq has been ranked as the fifth most vulnerable country to the phenomenon [5]. A major factor affecting human safety is climate change, which has caused disruptions in climatic resources like global temperature and precipitation patterns that have persisted for tens of millions of years on Earth [6]. These disruptions severely affected the global ecological

and biological growth systems that support human societies. According to the sixth Assessment Report (AR6) published by the Intergovernmental Panel on Climate Change (IPCC), the effects of climate change are unprecedented and irreversible. Over the current century, there could be a 1-3.5℃ increase in the average world temperature. The worldwide agricultural planting system and landscape will be greatly impacted by climate change, which will also cause enormous changes in space, time, and amount of climatic resources [7]. Long-term modifications to the Earth's climate, such as adjustments to temperature, precipitation patterns, and humidity, are referred to as climate change. Human activities like burning fossil fuels, deforestation, and industrial processes that emit greenhouse gases into the atmosphere are the main causes of it. These gases trap heat, which causes the Earth's climate system to be disrupted and the globe to overheat. Climate change is one of the most urgent global issues of our day since it affects ecosystems, weather patterns, sea levels, and human societies [8]. Both climate change and people's comfort levels are impacted by rising temperatures, particularly in urban areas. Temperature and humidity are two climate variables that are linked to people's degree of comfort. Human population comfort is gauged by several indices, such as the Temperature Humidity Index (THI) [9]. One of the axes of the applied climate research that has garnered significant interest over the years from academics, planners, and city people alike at the local, national, and international levels is the urban climate [10]. Increasingly effective analysis of satellite images (landsat8 OLI) and geographic information systems (GIS) have developed as an important tool for monitoring changes occurring in the environment [11]. Although the reliable data and depiction of climate change were fairly limited, scientific remote sensing technology allowed for the investigation and analysis of changes to every aspect of the climate [12]. Desertification is caused by rising temperatures and falling levels of precipitation, and is often accompanied by deterioration of the ecosystem. Thus, vegetation cover, as well as the absence of rain throughout the summer months in Iraq, are greatly influenced by the climate. Individuals in Amara City find the high temperatures and relative humidity uncomfortable [13]. Studies worldwide show that people feel most at ease in environments with clean air that fall within a certain range of temperatures and humidity. The impact of a planned urbanization area on human health is a key factor in determining whether a location is suitable for human habitation. The circumstances in which a person may adapt to their surroundings with the least energy use are known as bioclimatic comfort. The state of bioclimatic comfort is when an individual can adjust to their surroundings with the least energy [14].

Mariye et al. reported LULC classification and the perception of local people in Aykoleba, Northern Ethiopia. Utilizing remote sensing instruments and geographic information systems, the results demonstrated an assessment of the LULC categorization and an investigation of the factors influencing LULC change from 1973 to 2013. Over four decades, the analysis revealed a decrease in agricultural regions at the expense of land utilization [15]. Kadhim et al. studied the effect of temperature on land use and land cover LULC in Qalat Saleh. Using geographic information systems and remote sensing techniques, the study conducted in the Qalat al-Saleh area demonstrated the negative impacts of high temperatures on land use, agricultural land loss, and huge empty land. The area of vegetative cover shrank, and the amount of green space expanded as the temperatures increased [16].

In this research, the most suitable and severe heat discomfort were discussed. This is the first research that addresses these issues in the city of Amara. The analysis revealed a study of the elements of LULC, water, agriculture, barren areas, urban and industrial areas. In addition, the research included oil sites, as it analysed the study area for more than 30 years. The research problem is the random expansion of cities and urban areas at

the expense of agricultural areas and water and the increase in barren areas, which caused a lack of vegetation cover, an increase in temperatures and a lack of rain, as the elements of comfort lost in this region, making it one of the hottest cities in Iraq.

The research goals are: (1) to evaluate the LULC in Amara city, Missan province in southern Iraq during 1989-2023 using the Landsat 5 TM, Landsat 8 OLI and Landsat 9 OLI2 images, (2) to apply climate elements such as temperature and humidity and to evaluate the climatic suitability of the study area from 1990 to 2022.

1. 1. Study Area

Amara city is the administrative capital of Missan province, which is located in southeast Iraq. Missan lies between latitude (31° 50’ – 31° 83’ N) and longitude (47° 08’ – 47 14’ E). It is bordered to the north by Wasit province, to the south by Basra, and to the west by Dhi-Qar. Missan also represents a border governorate with Iran on its eastern border [17].

The alluvial plain that surrounds Missan is located in southeast Iraq. The region has a desert climate, with hot, dry summers and mild winters [18]. Fig. 1 shows the study area.

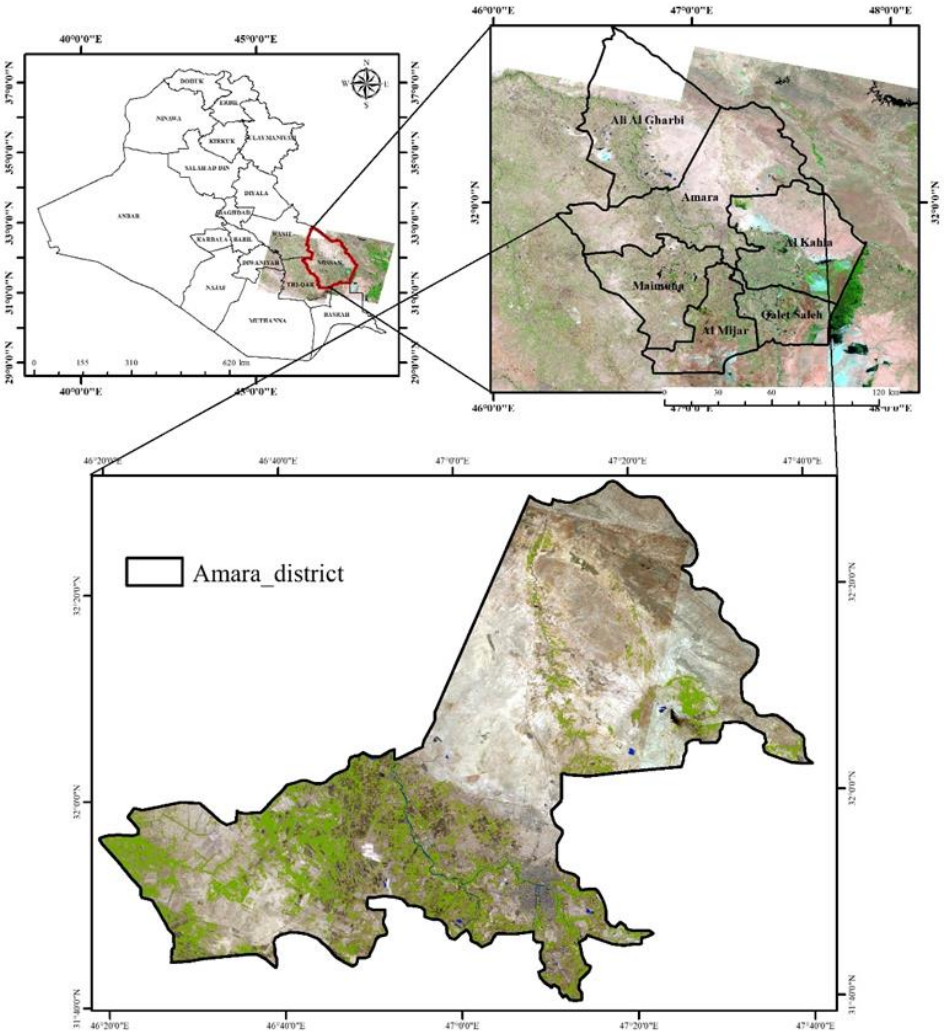

Figure 1: Location of the Amara city in Missan province.

2. Data Sources

For the purpose of this study, within clear skies devoid of clouds, Landsat images of Amara district were acquired in September. These images were taken from the USGS website [19]. They were characterized with a resolution of 30 m [20]. Landsat 5 images were taken on September 15, 1989, and September 19, 2000. While Landsat 8 images were acquired on September 30, 2013, and Landsat 9 images on September 18, 2023. Tables 1 and 2 show the wavelength bands of Landsat data.

Table 1: Details of bands landsat5 TM [21].

Band No.	Wavelength (μm)	Spatial Resolution (m)	Bands
1	0.45 - 0.52	30	Blue
2	0.52 - 0.60	30	Green
3	0.63 - 0.69	30	Red
4	0.77 - 0.90	30	NIR
5	1.55 - 1.75	30	MIR
6	10.40 - 12.50	120	Thermal
7	2.09 - 2.35	30	MIR

Table 2: Details of Landsat bands 8 OLI and Landsat 9 OLI2 [21].

Band No.	Wavelength (μm)	Spatial Resolution (m)	Bands
1	0.43 - 0.45	30	Coastal
2	0.45 - 0.51	30	Blue
3	0.53 - 0.59	30	Green
4	0.63 - 0.67	30	Red
5	0.85 - 0.88	30	NIR
6	1.57 - 1.65	30	SWIR1
7	2.11 - 2.29	30	SWIR2
8	0.50 - 0.68	15	Pan
9	1.36 - 1.38	30	Cirrus
10	10.60 - 10.19	100	TIRS1
11	10.50 - 12.51	100	TIRS2

The monthly temperature and humidity averages during 1990 – 2022 were used to evaluate the climatic suitability of Amara district. These data were obtained from the Iraqi Meteorological Organization and Seismology (IMOAS) (https://meteoseism.gov.iq).

Table 3 shows the monthly average temperatures from 1990 to 2022 obtained from the Meteorological Organization.

Table 4 shows the monthly average Relative Humidity % from 1990 to 2022 obtained from the Meteorological Organization.

Table 3: The monthly average temperatures(c) from 1990 to 2022.

STATION: AMARA					**Element: Mean Air Temp.(C)**							
YEAR	**JAN.**	**FEB.**	**MAR**	**APR**	**MAY**	**JUN**	**JUL**	**AUG**	**SEP**	**OCT**	**NOV**	**DEC**
1990	9.8	13.0	18.5	24.4	32.2	35.7	38.1	36.1	32.6	26.8	19.9	14.1
1991	11.0	13.6	18.0	24.8	30.8	35.4	36.9	35.8	31.9	26.1	19.8	12.8
1992	8.4	11.3	14.4	22.8	29.2	35.2	36.1	36.3	32.6	25.4	17.9	11.3
1993	10.1	12.7	17.1	23.6	29.5	35.2	37.4	36.6	32.6	26.5	17.2	14.7
1994	14.0	14.4	19.1	26.9	31.4	35.3	36.3	35.8	33.2	27.2	19.3	10.5
1995	12.6	15.0	18.9	23.9	31.6	35.6	36.7	36.7	31.7	25.7	18.0	12.1
1996	13.0	15.6	18.3	23.8	23.1	35.7	37.1	38.2	33.4	25.6	17.3	16.2
1997	12.7	11.4	16.0	23.6	32.2	36.9	37.1	35.6	32.7	27.2	19.1	13.0
1998	10.6	14.1	17.6	25.3	31.5	37.6	38.1	38.8	34.3	26.8	21.0	16.2
1999	13.0	15.2	18.8	26.2	32.9	37.1	37.8	38.8	34.0	28.6	18.4	12.8
2000	11.4	13.0	18.2	28.0	32.7	36.2	39.6	38.9	32.8	25.9	18.1	13.1
2001	12.2	14.1	18.5	27.1	32.8	36.7	38.7	38.9	33.4	27.3	18.3	13.0
2002	10.6	15.0	20.5	24.3	32.1	36.3	39.0	37.5	34.2	26.7	19.2	13.5
2003	10.7	14.0	19.0	24.5	31.7	36.0	38.7	37.6	33.8	27.0	19.3	11.5
2004	11.0	13.6	18.0	24.8	31.3	37.0	38.5	37.6	33.3	28.7	19.5	10.5
2005	12.2	13.6	19.1	25.6	38.1	36.0	39.3	38.0	33.4	26.1	16.4	15.7
2006	11.8	14.8	20.1	25.4	32.9	38.2	38.4	39.3	33.0	29.3	17.3	10.0
2007	9.7	15.3	18.3	24.2	33.3	37.2	38.2	38.4	34.4	28.5	19.2	12.7
2008	8.5	13.7	22.8	27.7	32.5	36.8	38.7	38.2	34.0	27.0	18.4	12.6
2009	11.0	15.5	19.0	23.9	32.4	37.0	38.1	36.8	33.0	27.5	19.1	15.3
2010	14.4	15.6	20.0	24.0	31.8	38.0	39.3	39.0	37.6	30.1	20.1	14.2
2011	13.0	14.0	20.1	20.0	33.0	36.0	39.0	38.2	33.5	26.1	16.5	14.3
2012	11.3	13.2	17.0	26.9	34.0	37.1	39.6	38.2	33.2	27.9	20.3	14.1
2013	11.2	14.1	185.0	27.4	31.1	35.7	38.5	36.1	33.1	25.0	18.8	12.0
2014	12.0	14.0	20.0	26.2	32.9	36.1	38.2	37.9	34.9	27.7	17.9	14.9
2015	13.0	15.7	20.4	26.2	33.7	37.6	39.7	39.9	35.6	29.0	18.6	12.2
2016	12.0	16.5	20.2	26.4	32.8	37.3	39.3	39.5	33.9	27.8	18.2	12.7
2017	12.2	12.6	20.0	26.7	32.9	37.7	39.9	39.7	36.0	28.7	20.7	15.2
2018	13.5	17.1	23.5	25.2	32.1	38	39.5	38.3	36.4	28.5	19.1	14.3
2019	12.6	14.7	17.8	23.3	32.9	38.6	38.9	39	35.9	29.6	19.1	14.3
2020	12.7	15.1	19.6	25.8	32.6	37.4	40.5	37.4	36	27.1	20.5	14
2021	13.2	16.2	20.7	28.4	35	38.3	40.6	39.3	34.6	28.4	21.4	15.1
2022	12	16.9	19.2	27.7	31.8	38.9	39.3	39.9	35	30	21.1	15.1
Ave. Temp.	11.7	14.4	24.1	25.3	32.1	36.8	38.5	37.9	33.9	27.4	18.9	13.5

Table 4: the monthly average Relative Humidity %.

STATION: AMARA					**Element: Relative Humidity %**							
YEAR	**JAN.**	**FEB.**	**MAR**	**APR**	**MAY**	**JUN**	**JUL**	**AUG**	**SEP**	**OCT**	**NOV**	**DEC**
1990	62	60	45	34	18	15	15	16	22	34	49	53
1991	67	65	55	45	25	30	30	29	35	54	60	78
1992	73	68	65	56	40	26	25	31	33	44	66	82
1993	80	73	63	63	47	29	28	32	31	45	62	69
1994	79	61	59	50	36	29	26	26	30	45	68	73
1995	77	71	61	58	39	32	27	25	33	41	50	66
1996	77	68	63	48	37	26	23	24	28	35	52	64
1997	69	55	59	46	32	25	22	24	28	46	71	82
1998	80	65	66	50	35	25	23	25	28	40	49	52
1999	69	64	56	43	34	26	26	24	32	39	56	74
2000	72	62	47	40	28	25	25	28	34	45	57	83
2001	76	67	59	44	32	24	23	27	29	39	50	73
2002	70	60	50	49	32	25	21	22	27	34	54	72
2003	70	60	50	48	36	24	21	21	26	34	55	70
2004	71	58	49	47	59	23	20	19	25	33	56	68
2005	72	56	49	46	30	22	19	23	26	36	56	69
2006	71	68	51	49	31	24	23	26	30	47	65	78
2007	78	64	55	51	35	27	24	24	27	40	47	63
2008	75	60	43	37	29	24	21	22	31	43	60	65
2009	62	60	52	48	33	23	22	25	30	40	60	73
2010	72	59	49	44	37	23	25	25	24	33	51	60
2011	70	62	48	32	32	26	17	23	28	30	53	61
2012	60	60	47	39	30	25	26	24	30	42	63	62
2013	62	63	43	38	37	28	23	26	31	42	70	72
2014	84	67	59	48	33	23	22	25	25	43	59	70
2015	65	64	50	34	27	20	20	22	29	40	66	72
2016	68	62	52	43	31	22	22	22	25	35	47	62
2017	59	49	51	32	32	22	21	23	26	36	51	54
2018	56	58	43	45	31	18	17	20	23	44	78	80
2019	76	67	59	54	37	25	21	22	26	38	55	78
2020	71	66	57	44	29	23	22	23	25	34	60	71
2021	64	62	51	37	27	21	20	21	25	31	50	66
2022	67	54	48	36	27	20	22	23	26	34	54	69
Ave. RH	70.4	62.4	53.2	44.8	33.3	24.2	22.5	24.0	28.1	39.3	57.6	69.2

3. Methodology

The following steps in Fig. 2 represents the methodology of the study:

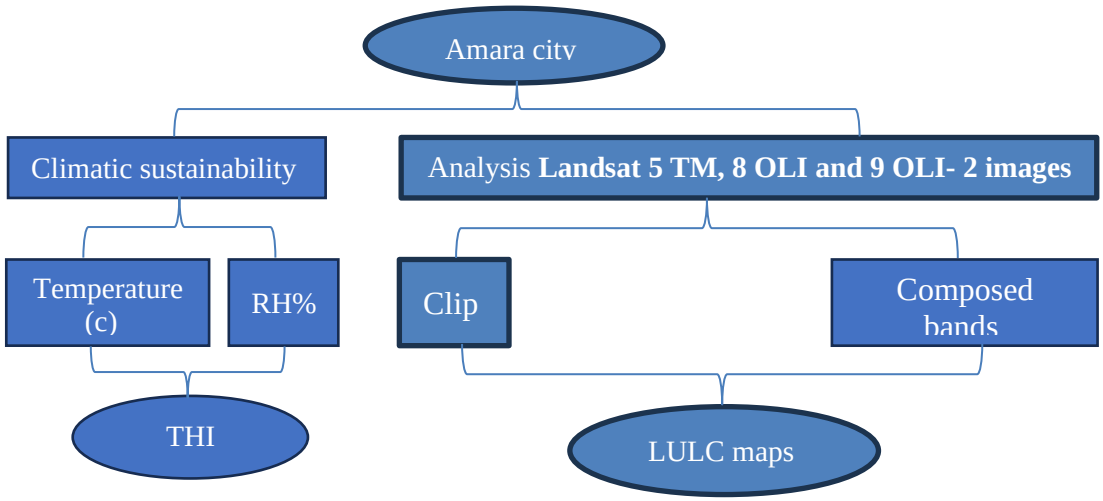

Figure 2: flow chart showing the steps for data processing and analysis.

3. 1. Specification Indices

3. 1. 1. Temperature-Humidity Indexes (THI)

A THI is a single number that combines the impacts of humidity and air temperature on the degree of thermal stress. This index was created as a weather safety measure to track and lessen losses caused by heat stress [22]. Several kinds of creatures, as well as, humans have distinct susceptibilities to air moisture content and ambient temperature. This index has been developed as a weather safety index to monitor and reduce heat stress-related losses [23].

The value of THI index can be calculated by the following equation [24]:

$$\mathrm{THI} = \mathrm{T} - 0.55 \times (1 - 0.01\mathrm{RH}) \times (\mathrm{T} - 14.5) \qquad (\mathbf{1})$$

where T is the temperature (°C), RH is relative humidity (%).

3. 1. 2. Unsupervised Classification Technique

Unsupervised categorization creates clusters based on the image's intrinsic spectral features that are similar. Next, Pixels are grouped using unlabeled data in unsupervised classification. The process of allocating pixels to raster data that is given in classes is known as image classification. Therefore, classifying land cover entails differentiating between distinct types of land cover using classification techniques that were created in the field of remote sensing [25].

4. Result and Discussion

4. 1. Land Use and Land Cover (LULC)

The LULC maps of the city of Amara for the years 1989, 2000, 2013, and 2023 are displayed in Fig. 3. For Amara city in 1989, Fig. 3 (A), the area of water and wetlands was estimated to be 72.8 km^2, distributed across several locations represented by the Amara River. Similarly, the Sabkha region registered 610.3 km^2. While agricultural areas were recorded to be 224 km^2. However, the barren area, which included large expanses to the east and west of Amara, recorded the highest area totaling 3560 km^2. The area of the city was 38.2 km^2. The population was largely concentrated in the center of the study area around the river, and agricultural areas were spread along the river and near bodies of water and marshes. Furthermore, the district's industrial area covered 18.8 km^2.

The LULC map, shown in Fig. 3 (B), is for Amara city in 2000. The results showed that, though small patches of water dispersed throughout the territory, the water area and wetlands totalled 43.1 km^2. Compared to 1989, the vegetation areas increased slightly to 255 km^2, while the area of Sabkha showed a slight increase to 655 km^2. Similarly, the barren area expanded to 3504.2 km^2 as a result of the drought that southern Iraq was experiencing at the time. Conversely, the industrial area grew somewhat to 24.4 km^2. Furthermore, the urban area grew to 44.4 km^2, spread in the city center.

The LULC map of Amara city in 2013 is depicted in Fig. 3 (C). According to the findings, it showed the lack of water area from 43.1 km^2 in 2000 to 37.5 km^2 in 2013 due to drought and the policies of neighboring governments, the area covered by vegetation greatly expanded to 810 km^2, and the area covered by Sabkha also somewhat decreased to 330 km^2. In 2013, due to urbanization and growing populations, urban and industrial areas grew to around 61 km^2 and 51.6 km^2, respectively. In addition to the industrial areas, oil fields were established east of the city, and its area was 26 km^2.

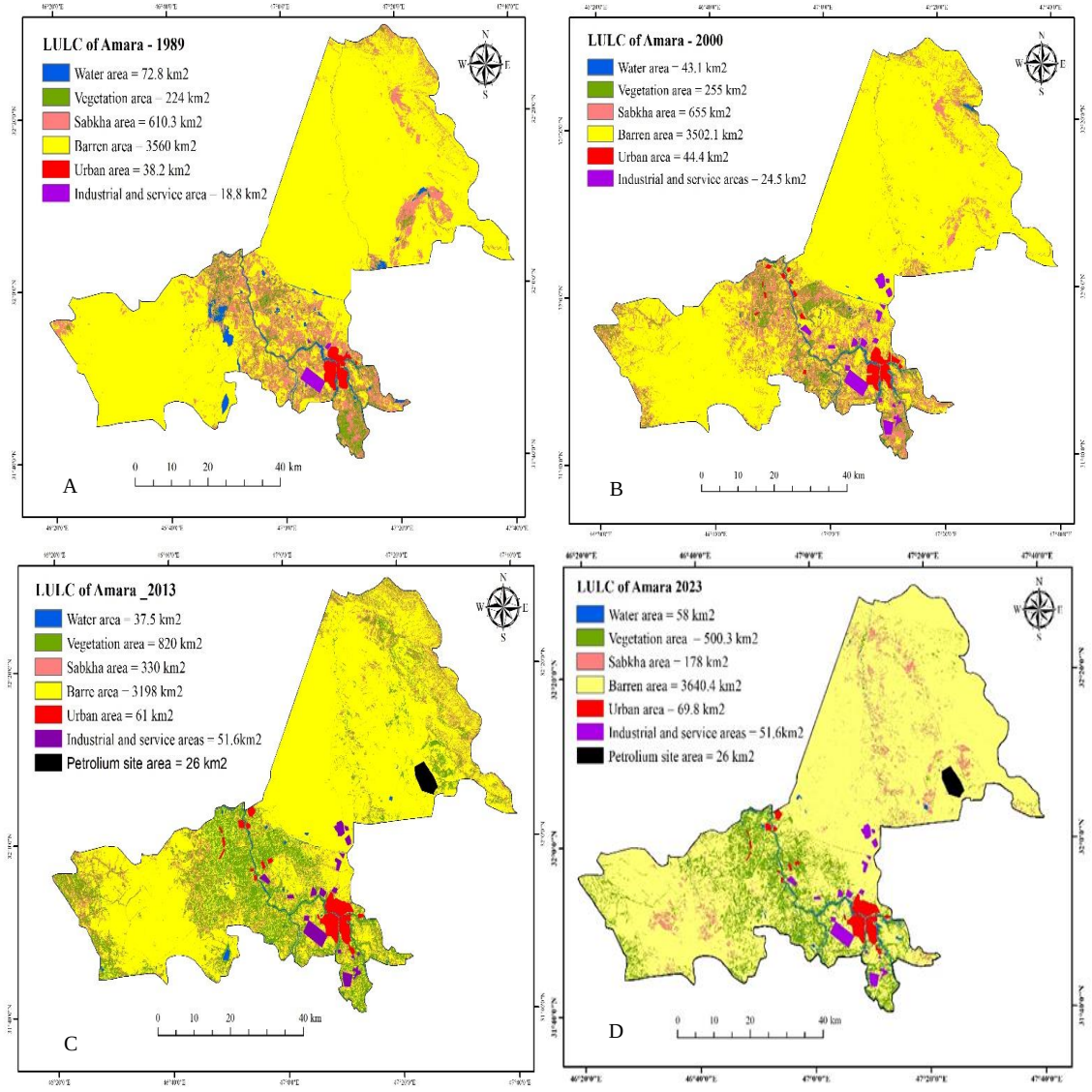

Figure 3: LULC (Land use Land cover) of Amara city (A) 1989, B) 2000, C)2013 and D) 2023).

Fig. 3 (D) depicts the LULC categories in Amara City in 2023. The area covered by wetlands and water rose marginally to 58 km^2, according to the results. The extent of vegetation covers and the area of Sabkha experienced a dramatic decline, with the former

measuring 500.3 km^2 and the latter 178 km^2. Urban areas are constantly growing by roughly 69.8 km^2. Due to low rainfall, high evaporation, and high temperatures, particularly in the southern sections of the country, Iraq has been experiencing a drought since 2019. This is the primary cause of the decline in water and plant areas and, therefore, increasing desert areas.

4. 2. Temperature and Humidity Index (THI)

The THI at Amara station was used in the current study to identify the months of comfort and discomfort. Additionally, the impact of each temperature and Relative Humidity (RH) on the temperature index values was examined. By computing the correlation coefficient, the relationship between temperature and humidity can be clarified. The monthly RH and temperature averages are displayed in Figs. 4 and 5, respectively. Fig. 4 displays the monthly temperature averages at the Amara station for 34 years from in 1990 to 2022. January had the lowest recorded temperature of 11.7°C, while July and August had the maximum temperatures of around 38.5°C and 37.9°C, respectively. The highest percentage of humidity was recorded, which shows the monthly humidity averages during the 34-year.

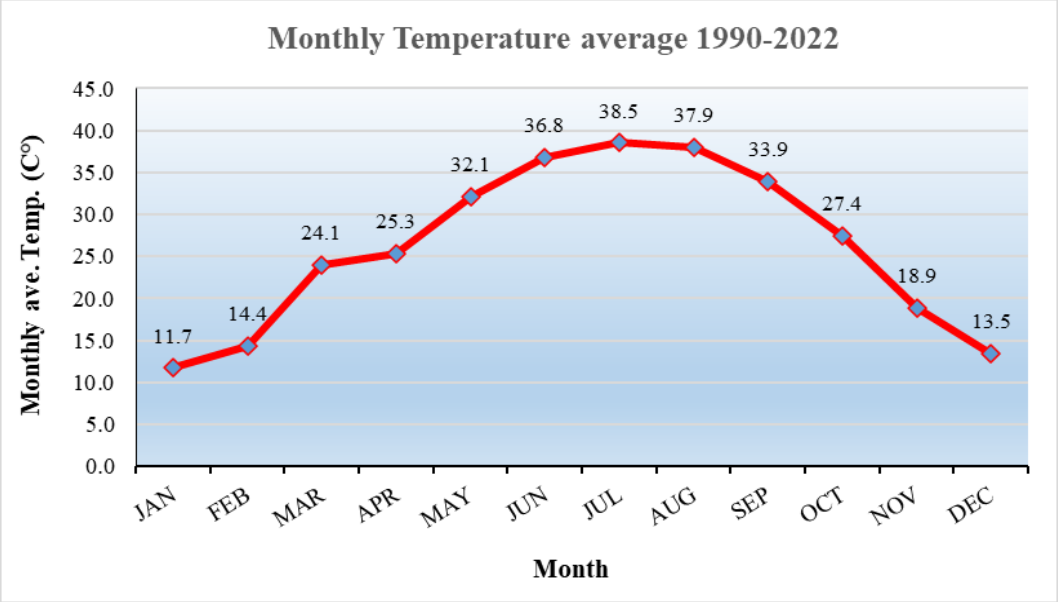

Figure 4: Monthly temperature averages in Amara station from 1990-2022.

Fig. 5 shows the monthly humidity averages during 34 years. The highest humidity levels were recorded in the months of January and February. The months of June, July and August recorded about 22 to 24% of relative humidity in January.

The values of the THI at Amara station from 1990 to 2022 are displayed in Table 4 and Fig. 6.

According to the humidity values in the table and graph, January, February, and December were the most uncomfortable due to the cold, while March and April months of the year were cool. In contrast, June, July, and August were extremely uncomfortable due to heat, and May and September months of the year were uncomfortable due to heat.

Only three months, March, April, and November, were both comfortable and cool based on the THI values in the chart. The two months that were uncomfortable owing to coldness were January and February. Conversely, May and September were quite hot, while June, July, and August were three unbearably hot months. The THI index has two recorded values: a maximum of 28.27 in July and a minimum of 12.1 in January. Based on the THI standards, it was noted that there were no months of complete rest in the values

of THI in Amara city because the category of complete rest ranged from 17.8 to 21.6. Based on the monthly temperature and relative humidity averages at the Amara station, no comfortable month was recorded in Amara city between 1990 and 2022. The months of discomfort that the city of Amara documented in relation to the THI equation and guide were caused by temperature and RH values that exceeded the ranges appropriate for human body comfort and activity. These ranges are 18–28 C° for temperature and 40–60% for RH.

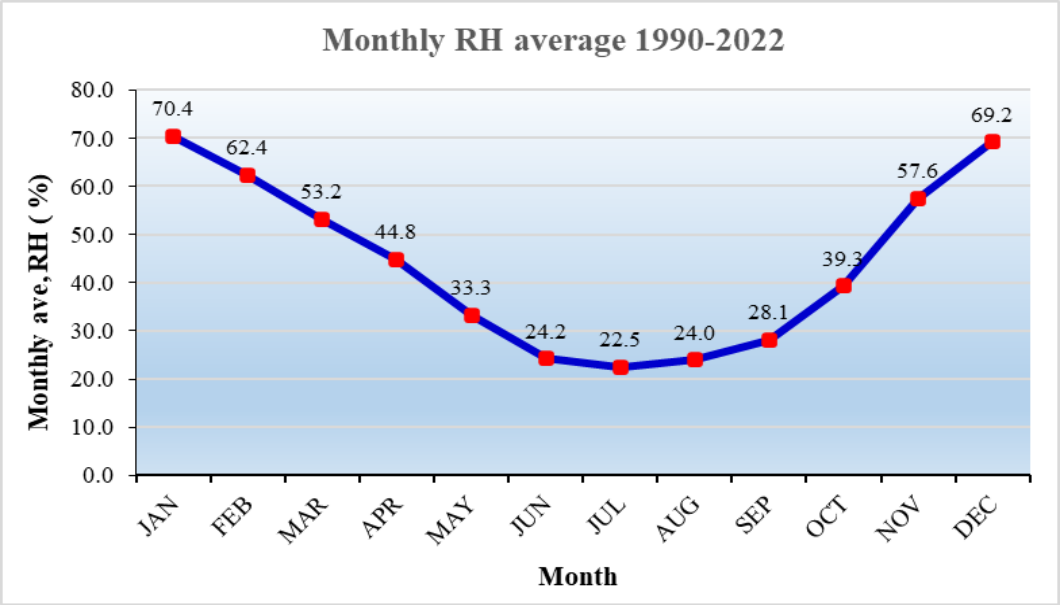

Figure 5: Monthly RH averages in Amara station from 1990-2022.

Table 4: THI values at Amara Station from 1990-2022.

Months	THI	Symbols	Climate sense
Jan.	12.1	C	Cold discomfort
Feb.	14.4	C	Cold discomfort
Mar.	21.6	P+	Thermal comfort
Apr.	22	P+	Thermal comfort
May.	25.6	H	Feverish discomfort
Jun.	27.5	H+	Severe heat discomfort
Jul.	28.27	H+	Severe heat discomfort
Aug.	28.11	H+	Severe heat discomfort
Sep.	26.22	H	Feverish discomfort
Oct.	23	P+	Thermal comfort
Nov.	17.8	P-	Cool comfort
Dec.	13.6	P-	Cool comfort

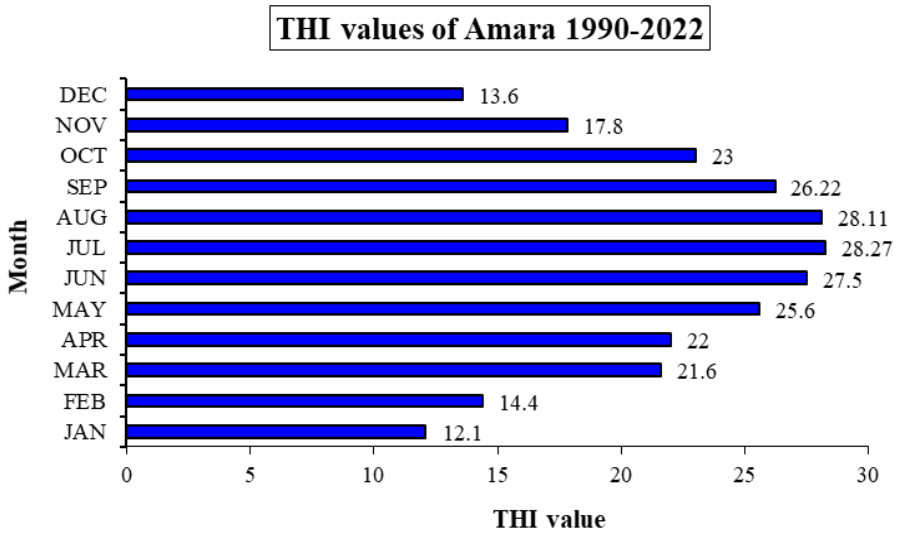

Figure 6: THI values at Amara station between 1990 and 2022.

4. 3. Correlation relationships between temperature and THI value

The relationship between the monthly temperature averages and THI values for Amara city from 1990 to 2022 is depicted in Fig. 7. The findings showed a strong positive association, with a correlation coefficient of about (r = 0.98). On the other hand, the relationship between monthly temperature averages and THI values, shown in Fig. 8, exhibited a strong negative connection (r = 0.96) between the RH and THI values. These findings support the fact that there is an inverse relationship between RH and THI values and a direct relationship between temperature and THI values.

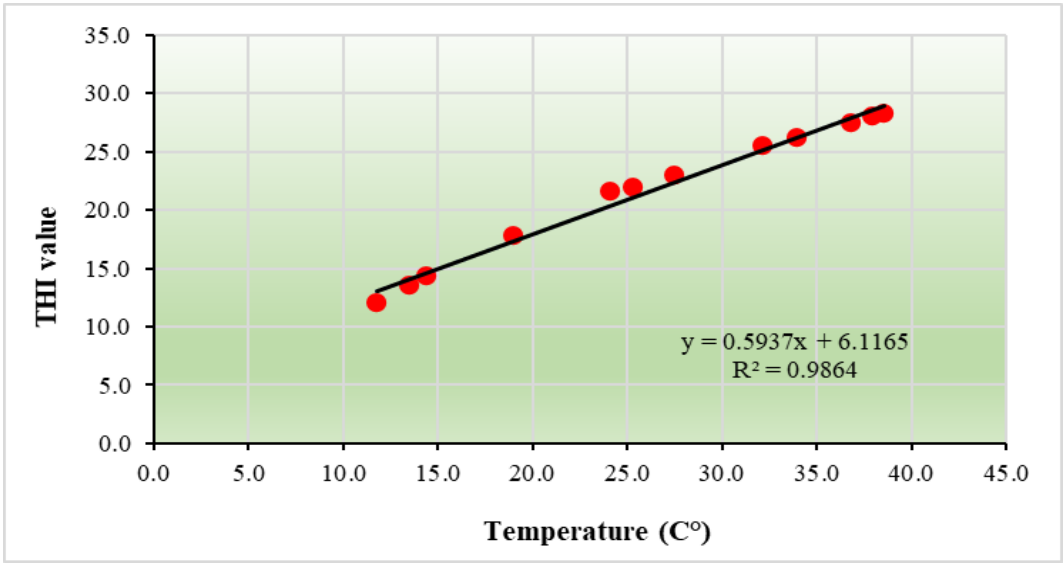

Figure 7: The correlation relationship between the monthly temperature averages with THI values for Amara city during1990-2022.

The findings were consistent with those of other researchers: water regions shrank while residential and barren areas grew in size. There was a little increase in the areas covered by vegetation. The findings from this study and those of other researchers are listed in the section on earlier studies are displayed in Tables 5 and 6.

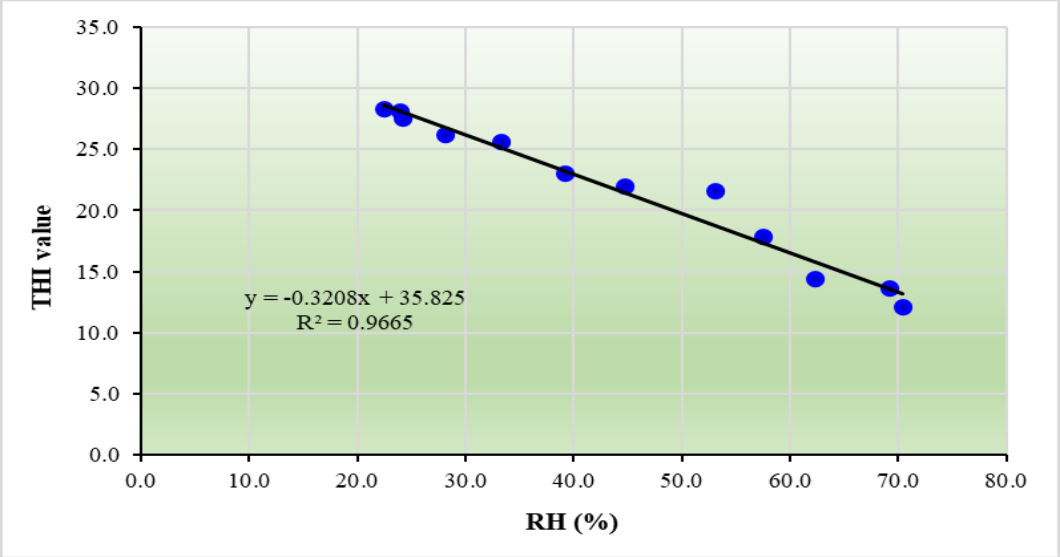

Figure 8: The correlation relationship between the monthly RH averages with THI values for Amara city during 1990-2022.

Table 5: The (LULC) areas of Amara city during a forty-year period (1989.2000.2013 and 2024).

Categories	Area km²		Area km²	
	1989	2000	2013	2023
Water	72.8	43.1	37.5	58
Vegetation	224	255	820	500.3
Sabkha	610.3	655	330	178
Barren	3560	3502.1	3198	3640.4
Urban	38.2	44.4	61	69.8
Industrial	18.8	24.5	51.6	51.6
Petroleum	-	-	26	26

One of the researchers in Table 6 studied land use in Qalaat Saleh in Missan Governorate, and his results were consistent with the results of this study. The area of water decreased, it indicates a slight increase in the area of agricultural land, as well as an increase in built-up and barren areas.

Table 6: Types of (LULC) in the Qalaa Saleh district during the time period (2013-2023).

Categories LULC	Area km ² 2013	Area km ² 2023
Water bodies	301.8	102.33
Agriculture land	402.7	445.12
Built up area	99.9	148.07
Barren land	344.8	453.89

5. Conclusions

New developments in remote sensing methods provide an effective tool for creating unique LULC maps. The study area, which was studied from 1989 to 2023, was characterized by a higher percentage of arid regions, a lack of water area, and a lack of vegetation cover. Urban areas require sustainable urban planning as they have grown from 38.2 to 69.8 in 34 years. Based on the results discussed above, it can be concluded that the city suffers the highest temperatures between June and September, with June, July, and August being the climax of the climate. The colder months are January and February, with November and December being the rest months with a tendency for chilly weather.

Conversely, June, July, and August were noted as the hottest months, with March, April, and October exhibiting a moderate level of heat. The THI values for the hottest months were (27.5, 28.27, 28.11), while January having the lowest value (12.1). For the city of Amara, the monthly average temperatures and THI values showed a strong positive correlation with a value of 0.98. The humidity and THI values confirmed a strong negative relationship with a value of 0.96, where the relationship between humidity and THI has a strong negative correlation, while temperature and THI have a strong positive relationship.

Acknowledgments

The authors would like to express their gratitude to the University of Baghdad, College of Science, Remote Sensing Unit and the Department of Remote Sensing and GIS for their support.

Conflict of interest

Authors declare that they have no conflict of interest.

References

1. A. I. Hamad, A. B. Ali, and A. F. Hassoon, AIP Conf. Proc. **2398**, 020055 (2022). DOI: 10.1063/5.0097668.
2. S. S. Saud, S. A. Abdullah, and B. Mohammed Hashim, Iraqi J. Phys. **21**, 66 (2023). DOI: 10.30723/ijp.v21i4.1155.
3. M. F. Allawai and B. A. Ahmed, IOP Conf. Ser.: Mater. Sci. Eng. **757**, 012062 (2020). DOI: 10.1088/1757-899X/757/1/012062.
4. A. Gafurov, V. Prokhorov, M. Kozhevnikova, and B. Usmanov, Remote Sens. **16**, 1371 (2024). DOI: 10.3390/rs16081371.
5. A. M. F. Al-Quraishi, Y. T. Mustafa, and A. M. Negm, *Environmental Degradation in Asia: Land Degradation, Environmental Contamination, and Human Activities* (Iraq, Springer Nature, 2022).
6. A. M. F. Al-Quraishi and A. M. Negm, *Environmental Remote Sensing and Gis in Iraq* (Iraq, Springer 2020).
7. B. M. Hashim, M. A. Sultan, M. N. Attyia, A. A. Al Maliki, and N. Al-Ansari, Appl. Sci. **9**, 2016 (2019). DOI: 10.3390/app9102016.
8. N. Adamo, N. Al-Ansari, V. Sissakian, K. J. Fahmi, and S. A. Abed, Engineering **14**, 235 (2022). DOI: 10.4236/eng.2022.147021.
9. S. Ramdhoni, S. B. Rushayati, and L. B. Prasetyo, Proced. Envir. Sci. **33**, 204 (2016). DOI: 10.1016/j.proenv.2016.03.071.
10. S. A. Abdullah and T. R. Aziz, J. Phys.: Conf. Ser. **2114**, 012024 (2021). DOI: 10.1088/1742-6596/2114/1/012024.
11. F. H. Mahmood and G. S. Al-Hassany, Iraqi J. Sci. **55**, 1663 (2014).
12. R. Al-Hakeem and Y. a.-K. Qusai, Iraqi J. Phy. **20**, 10 (2022). DOI: 10.30723/ijp.v20i4.1021.
13. S. A. Abdullah Albakri, M. N. A. Hussien, and H. Herdan, IOP Conf. Ser.: Mater. Sci. Eng. **757**, 012043 (2020). DOI: 10.1088/1757-899X/757/1/012043.
14. L. M. Irimia, C. V. Patriche, H. Quenol, L. Sfîcă, and C. Foss, Theor. Appl. Climat. **131**, 1069 (2018). DOI: 10.1007/s00704-017-2033-9.
15. M. Mariye, M. Maryo, and J. Li, African J. Envir. Sci. Tech. **15**, 282 (2021). DOI: 10.5897/AJEST2021.3022.
16. S. H. Kadhim, S. M. Al-Jawari, and N. A. Razak Hasach, Int. J. Sustain. Develop. Plan. **19**, 123 (2024). DOI: 10.18280/ijsdp.190110
17. M. A. Almusawi and H. S. Obaid, Misan J. of Acad. Stud. **21**, 188 (2022). DOI: 10.54633/2333-021-043-013.
18. M. K. A. Al-Jabri and E. I. Ladik, IOP Conf. Ser.: Earth Environ. Sci. **1129**, 012013 (2023). DOI: 10.1088/1755-1315/1129/1/012013.
19. The Act of Congress. *United States Geology Survey (Usgs)*; https://www.usgs.gov/.
20. B. M. Hashim, A. Al Maliki, M. A. Sultan, S. Shahid, and Z. M. Yaseen, Nat. Haz. **112**, 1223 (2022). DOI: 10.1007/s11069-022-05224-y.
21. S. S. Saud, S. A. Abdullah, and B. M. Hashim, IOP Conf. Ser.: Earth Environ. Sci. **1202**, 012013 (2023). DOI: 10.1088/1755-1315/1202/1/012013.

22. E. F. Khanger, B. A. Al Razaq, R. R. Ismail, and Z. F. Rasheed, IOP Conf. Ser.: Mater. Sci. Eng. **757**, 012030 (2020). DOI: 10.1088/1757-899X/757/1/012030.
23. A. Musari, O. Sojobi, O. Abatan, and A. Egunjobi, IOSR J. Appl. Phys. **7**, 60 (2015). DOI: 10.9790/4861-07116066
24. J. H. Mohammed, Kirkuk Univ. J. Sci. Stud. **15**, 87 (2020). DOI: 10.32894/kujss.2021.167519.
25. E. S. Hassan, A. F. Hasson, and E. F. Khanjer, IOP Conf. Ser.: Earth Environ. Sci. **1223**, 012023 (2023). DOI: 10.1088/1755-1315/1223/1/012023.

تقييم الملاءمة المناخية مع توزيع الغطاء الأرضي لمدينة العمارة باستخدام تقنيات الاستشعار عن بعد

هوازن حسن مسلم[1] وباسم محمد هاشم[2] وسندس عبد العباس عبدالله[1]

[1]التحسس النائي ونظم المعلومات الجغرافية، العلوم، جامعة بغداد، بغداد، العراق

[2]مركز بحوث وتكنولوجيا البيئة والمياه والطاقات المتجددة، هيئة البحث العلمي، وزارة التعليم العالي والبحث العلمي، بغداد، العراق

الخلاصة

استخدمت الدراسة الحالية بيانات الأقمار الصناعية ونظام المعلومات الجغرافية لكشف التغيرات في استخدامات الأراضي والغطاء الأرضي وأيضا دراسة العوامل المناخية درجة الحرارة والرطوبة في مدينة العمارة التي تقع في جنوب شرق العراق من عام 1990 إلى عام 2022. هدفت الدراسة إلى حساب LULC باستخدام صور الأقمار الصناعية Landsat5 TM وLandsat 8 OLI وLandsat 9 OLI2، وأيضًا من هيئة الأرصاد الجوية تم الحصول على بيانات درجة الحرارة والرطوبة المستخدمة لحساب مؤشر THI بمعادلة خاصة. لقد كان العراق من أكثر الدول التي تعرضت لتغير المناخ نتيجة ظاهرة الاحتباس الحراري وآثارها. كانت هناك حاجة ملحة للبحث في دراسة عناصر المناخ واستخدام الأراضي في مدينة العمارة مع ارتفاع درجات الحرارة وتعرض المدينة للجفاف ونقص هطول الأمطار. وأظهرت النتائج أن نسبة المساحة الحضرية زادت بشكل ملحوظ من 38.2 كم^2 إلى 69.8 كم^2، وتزايدت كمية الغطاء النباتي بشكل طفيف، وكانت المناطق القاحلة هي الأعلى. يعد انخفاض هطول الأمطار في منطقة الدراسة وارتفاع درجات الحرارة الناجم عن ظاهرة الاحتباس الحراري من المتغيرات الرئيسية التي تؤثر على السلامة العامة، والعوامل الرئيسية التي تؤثر على راحة السكان هي درجة الحرارة والرطوبة. كما أشارت نتائج ملاءمة المناخ إلى أن شهري نوفمبر وديسمبر يعتبران الأشهر الأكثر ملاءمة للسكان، في حين كانت الأشهر الأكثر حرارة والأكثر إزعاجاً هي الفترة من نهاية مايو إلى بداية سبتمبر.

الكلمات المفتاحية: استخدامات الارض، الغطاء الارضي، قمر صناعي، مؤشر درجة الحرارة والرطوبة، الموائمة المناخية.